



Original Articles

Suspended-sediment transport related to ice-cover conditions during cold and warm winters, Toudaoguai stretch of the Yellow River, Inner Mongolia, China

Shuixia Zhao^{a,b,*}, Quancheng Zhou^a, Wenjun Wang^a, Yingjie Wu^a, Chao Li^c, Qiang Quan^a, Parisa Radan^d, Youcai Tuo^e, Tomasz Kolerski^{d,*}

^a Yinshanbeilu Grassland Eco-hydrology National Observation and Research Station, State Key Laboratory of Simulation and Regulation of Water Cycle in River Basin, China Institute of Water Resources and Hydropower Research, Beijing 100038, China

^b Institute of Water Resources for Pastoral Area, Ministry of Water Resources, Inner Mongolia Hohhot 010020, China

^c College of Water Conservancy and Civil Engineering, Inner Mongolia Agricultural University, Inner Mongolia Hohhot 010018, China

^d Department of Civil and Environmental Engineering, Gdańsk University of Technology, 80-233 Gdańsk, Poland

^e State Key Laboratory of Hydraulics and Mountain River Engineering, Sichuan University, Chengdu 610065, China



ARTICLE INFO

Keywords:

Climate change
Cold and warm winter
Ice regime characteristic
Sediment concentration
Inner Mongolia reaches

ABSTRACT

The presence of winter ice in cold regions changes the water level, flow rate, velocity distribution, and other parameters of the river, which in turn affects the sediment concentration and channel evolution. Based on data obtained from Toudaoguai Hydrological Station from 1959 to 2021, this study examines the characteristics of the ice regime during cold and warm winters and the water and sediment transport processes along the Yellow River in Inner Mongolia in the context of climate change. The Mann–Kendall test and trend analysis were applied to define the years of temperature mutations and their trends, and the temperature mutation point was determined to be the 1987/1988 season. The study considers the effect of climate change on the combination of hydrological and hydraulic conditions. Therefore, trends in suspended sediment transport, ice type formation, water discharge, and storage in different ice flood seasons (November 1 to March 31, from 1998 to 2021) were attained. Based on the cumulative negative air temperature, winters were categorized into three types, warm, normal, and cold (52.2%, 17.4%, and 30.4%, respectively). Strong and weak grades further divide cold and warm winters, and statistical analyses were used to examine the characteristics of ice, water discharge, channel storage, and sediment transport. The duration of open water, freeze-up, ice cover, and breakup periods were calculated, and the relationship between the suspended sediment transport rate and discharge rate in these various ice periods was defined. The obtained relations show that the suspended sediment rate during the ice cover and first drift was smaller than that during the open water and post-breakup conditions. For the ice cover period, the sediment transport rate was on average approximately four times smaller than the freeze-up condition and six times smaller than the open water condition. The reduced sediment transport rate in the freeze-up period can be attributed to the weakened vertical turbulent mixing and increased flow resistance.

1. Introduction

As the climate changes, the occurrence, timing, and severity of different types of winter climates (cold, normal, and warm) will change. Changes in cold and warm winter climates have an important impact on river and ice flow characteristics. These, in turn, affect riverbed evolution, river course stability, and water resource allocation. Understanding

changes in ice formation, runoff, and sediment flow characteristics during different types of winter has important practical significance for flood prevention and soil erosion control throughout the basin (Wang et al., 2016). Global warming is an undeniable phenomenon. In the mid-1980s, following annual temperature rises through the 1960s and temperature stabilization in the 1970s, the winter temperature in China began to increase at a rate significantly higher than that of other seasons

* Corresponding authors at: Institute of Water Resources for Pastoral Area, Ministry of Water Resources, Inner Mongolia Hohhot 010020, China (S. Zhao); Department of Civil and Environmental Engineering, Gdańsk University of Technology, 80-233 Gdańsk, Poland (T. Kolerski).

E-mail addresses: zhaosx@iwhr.com (S. Zhao), zhouqch@iwhr.com (Q. Zhou), tomasz.kolerski@pg.edu.pl (T. Kolerski).

<https://doi.org/10.1016/j.ecolind.2023.110435>

Received 12 January 2023; Received in revised form 6 April 2023; Accepted 22 May 2023

Available online 3 June 2023

1470-160X/© 2023 The Author(s). Published by Elsevier Ltd. This is an open access article under the CC BY license (<http://creativecommons.org/licenses/by/4.0/>).

(He, 2013; You et al., 2010). Annual warming can be mostly attributed to increased temperature in the autumn and winter (You et al., 2010). The warmer winter climate is owing to a combination of natural factors and human activities; in terms of natural factors, it is mainly related to the East Asian winter monsoon, the Western Pacific subtropical high, the El Niño-Southern Oscillation phenomenon, and Eurasian snow cover (Chen et al., 2013). Owing to the comprehensive impact of multiple factors and unusual temperature fluctuations, regional cold winters have also occurred sporadically in China (You et al., 2010; Zhang et al., 2013).

Kämäri et al. (2015) analyzed the sediment transport process along a river course with and without ice covers. They found that the presence of ice covers decreased the amount of suspended sediment along the river course. By contrast, the sediment transport rate decreased in areas with lower flow rates. An increase in air temperature can shorten the ice cover period and increase river flow in the winter, thus, increasing the erosion potential of the riverbed and the quantity of transported and silted sediment during winter. Turcotte et al. (2011) explored the impact of river ice processes, ice jams, and hanging dams on sediment transport in a river. They concluded that the riverbank freeze-thaw cycle in winter increased the sediment supply along the river course. The existence of stable ice covers reduces the suspended sediment transport capacity of the river. The influence of ice jams on sediment transport also leads to decreased conveyance in the water flow, thus, increasing sediment deposition in the backwater area. Additionally, water velocity at the ice jam toe increases, causing scouring in this section (Ettema, 2006; Prowse, 2001). Knack and Shen (2015, 2018) reviewed the transport characteristics of sediment under an ice cover using laboratory experiments. They propose using the modified Rouse equation to calculate the transported suspended mass under an ice cover and a two-dimensional coupling model of river ice and sediment. Studies in China have used the field prototype monitoring test for sediment and ice regimes. These studies conclude that the change in the flow process caused by river ice along the river course is an important factor affecting sediment content (Polvi et al., 2020; Sui et al., 2000). Frazil ice accumulation under ice jams correlates with riverbed scouring and sedimentation and is consistent with the flow rate distribution and development trend (Gao et al., 2019). Fu et al. (2007) systematically summarize progress on understanding sediment transport during the freeze-up period and investigated the sediment load carried by frazil ice. By further examination of the initial flow rate of sediment during ice cover flow using the flume test, they discovered that the bed load and suspended sediment transport rates under the ice cover were lower than those of an identical open flow rate. The sediment flow rate under the ice cover was significantly lower than that under open flow. The magnitude of difference depends on the ratio of ice cover roughness to bed surface roughness (Decker and Leonard, 2004; Wang and Sun, 1998).

Thus, although previous studies have established a foundation of knowledge on the interactions between river ice and sediment in winter, the interaction mechanism remains unclear. Few studies have focused on the law of ice regime, water, and sediment transport in cold and warm winters in the context of climate change.

Owing to the geographical features of the basin, meandering course, and strong cold air function in winter, ice jams and associated flooding of varying degrees occur along the Inner Mongolian reach of the river. Compared with the open-channel-flow period, during the winter period, significant changes in hydraulic features, riverbed scouring, and silting evolution occur (Ji et al., 2019; Wang et al., 2016). Additionally, the Inner Mongolian reach along the main channel of the river is characterized by active wind and runoff erosion. Sandy terrain in the northern part of the Ordos Plateau and the “Ten Watersheds” on the southern bank of the river affect the variability of the water and sediment sources along the river and sediment silting, which in turn have substantially affected the risk of river flooding during winter (Tian et al., 2022; Wang et al., 2016). Complex changes during periods of ice formation, growth, and breakup affect river-sediment loads, which in some instances can

change channel morphology and, thus, in-channel flow conveyance, thereby affecting the occurrence of flood events, especially in narrow and severely deposited channels. The interaction between ice flood occurrence and channel erosion significantly increases the difficulty of investigating ice phenomena, river hydrodynamic changes, and sediment characteristics in the context of climatic change.

As a comprehensive representation of thermal factors, temperature is the key factor that determines the occurrence and development of flooding in the Yellow River. Repeated fluctuations in temperature impact the processes and types of freeze-up and breakup (Ettema, 2002). The abnormal rise in temperature in this region began in the winter of 1987/1988; as a result, the average temperature along the river reaches has increased during the ice flood season. The winter of 1998/1999 was a 1:500 annual exceedance probability (AEP) warm winter in Inner Mongolia (Du et al., 2014). Consequently, the ice regime was influenced by relatively high temperatures during the freeze-up period, delayed freeze-up, and thin ice in comparison to those during the average temperature condition in this period. The winter of 1999/2000 was reported to be colder than the previous 20 winters. This winter was characterized by the farthest downstream extension of the initiation of the cover formation, a long frozen reach, thick ice layer, and increased water storage in the channel (Quan et al., 2018; Zhang and Lu, 2021). Owing to warming, shorter ice seasons are observed, although the warm winters increase the uncertainty related to ice processes, causing more violent ice breakups and flooding (Beltaos and Prowse, 2009). A comprehensive understanding of this phenomenon is required considering the variation in mutual relations between hydraulic, hydrological, and morphological characteristics owing to climatic changes.

Therefore, the goal of this study is to enhance the understanding of changes in river flow, ice, and sediment regimes of the Inner Mongolian reaches of the Yellow River during different types of winter climates considering the effects of climatic change. The Inner Mongolian reaches of the Yellow River, China was considered for understanding the combination of these parameters as a case study. These reaches are located at the northern end of the Yellow River Basin, which is an important surface water resource and ecological site in North China. The hydro-meteorological data from Toudaoguai Hydrological Station of the Yellow River in Inner Mongolia from 1959 to 2021 is adopted, which controlled a catchment area of 367898 km². The specific study period is November 1 to March 31 of each year, which is known as the ice flood season. Temperature changes were considered, and winters were classified by type. In addition, the ice regime, flow rate, and sediment transport characteristics of typical flood-disaster reaches during different winters were explored in the context of climate change.

2. Study area overview

The Inner Mongolian reaches of the main channel of the Yellow River (Fig. 1) are located at the northern end of the Yellow River Basin, beginning at Shizuishan in Ningxia and ending at Jungar Banner in Ordos City, Inner Mongolia. The river is 840 km long and has a large curve similar to the shape of the Chinese character “Ji.” It is characterized by an arid and semi-arid, temperate continental climate, with an average multi-year temperature of 9 °C, large temperature differences, and clear seasonal variations. Controlled by the Siberian High, the winters in this area are cold and long, with frozen periods lasting 4–5 months. The unique high-latitude climate characteristics and complex river sinuosity in Inner Mongolia can easily lead to sudden ice jams and dams during the ice period. Reservoirs are considered as efficient flood mitigating methods, in the sense of controlling flow distribution in ice flood seasons. Between 1952 and 2017, the maximum, minimum, and multi-year mean water discharges during winter in Inner Mongolia reaches of Yellow River were 953 m³/s (in 1990), 62.1 m³/s (in 1986), and 589 m³/s, respectively.

The Toudaoguai Hydrological Station is situated in Tuoketuo County, and is the last gauging station on the upper reach of the Yellow

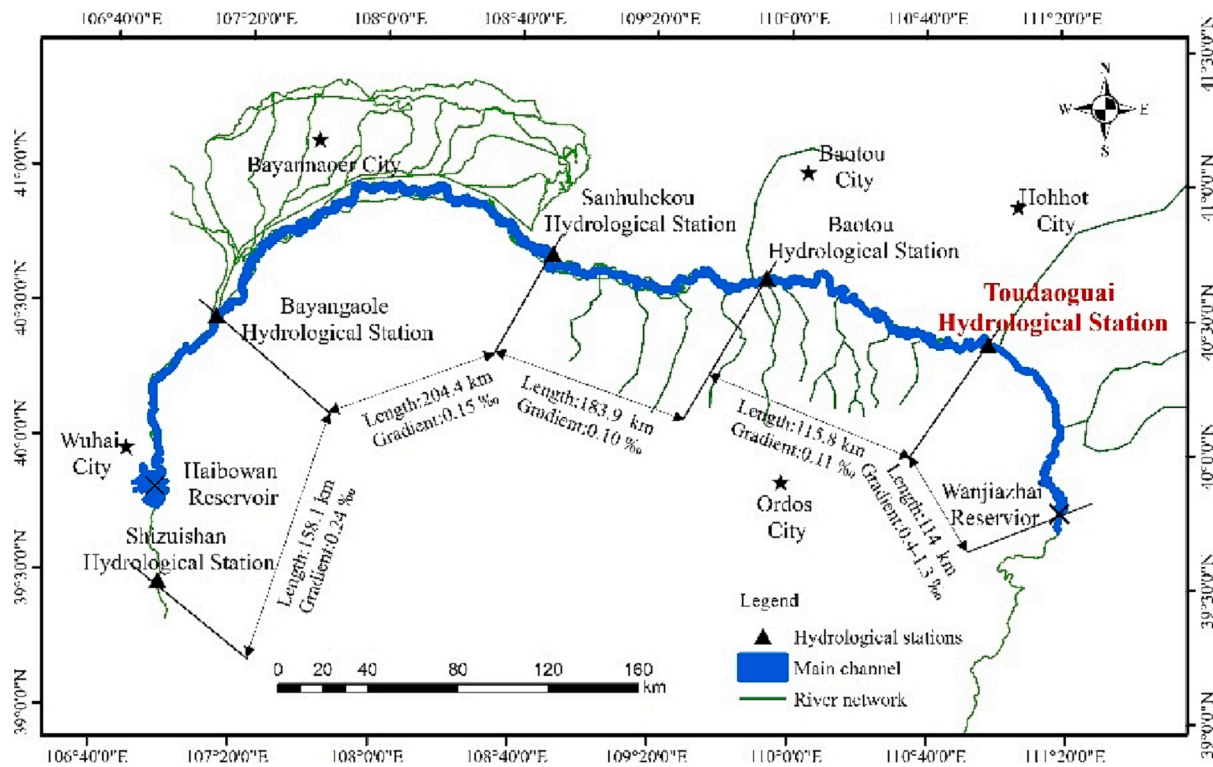


Fig. 1. Geographical location of the main channel of the Yellow River and Toudaoguai Hydrological Station in Inner Mongolia. (For interpretation of the references to colour in this figure legend, the reader is referred to the web version of this article.)

River. It is the main monitoring station for the collection of data regarding discharge, sediment load in the upper and middle reaches of the Yellow River, as well as information on the ice regime. The annual rainfall at this station is 155–366 mm. The average annual runoff and sediment discharge are 33.7 billion m³ and 102.2 million tons, respectively, accounting for approximately 63 % of the natural runoff into the Yellow River Basin and 6.4 % of the total sediment transport of the river (Ran et al., 2015). Due to river morphology and climatic conditions, the reach is prone to ice jamming and consequent flooding (Ran et al., 2015; Zhao et al., 2017). The upper part of the Toudaoguai reach is a plain, characterized by wide and shallow courses and slow water flow, while the lower part is a canyon, characterized by narrow and deep courses of rapid water flow. The different morphological characteristics of the upper and lower sections lead to notable changes in river flow, i.e., they are mostly caused by the variations in bed slope. The unregulated discharge and sediment flow also lead to shrinking river courses, riverbed deposition, and a reduction in the runoff and sediment conveyance capacity during the frozen period (Zhao et al., 2016). This increases the frequency of flood occurrence, complicating the ice, water, and sediment transport along the river courses. The data on daily average air temperature, water discharge, sediment concentration, and ice condition are obtained from the official water regime bulletin and sediment bulletin of the Yellow River Conservancy Commission of the Ministry of Water Resources (<https://www.yrcc.gov.cn/>). Daily measurements of air temperature and water surface elevation are conducted, while water discharge is calculated based on the rating curve and sediment concentration based on collected water samples.

3. Methods

Trend and Mann–Kendall (M-K) mutation tests on the cumulative negative air temperature were used to analyze climate change processes and obtain the mutation year for Toudaoguai Hydrological Station from 1959 to 2021. The cumulative negative air temperature is the sum of the daily mean air temperature from November 1 to March 31 when it turns

negative over the positive temperature periods over the 62 year period. Since this hydrological and meteorological data sample is not distributed by outliers, the M-K test can be used as an approach for applying the mutation test (Paul et al., 2017).

Assuming the sample size of the cumulative negative air temperature time series ($X = \{x_1, x_2, \dots, x_n\}$) is n , a statistical variable, S_k , which is the cumulative value of the negative temperature can be obtained, under the condition of the i -th value of the time series is greater than that of the j -th value:

$$S_k = \sum_{i=1}^k r_i, k = 2, 3, \dots, n \tag{1}$$

and

$$r_i = \begin{cases} 1, & \text{when } x_i > x_j \quad (j = 1, 2, \dots, i) \\ 0, & \text{when } x_i \leq x_j \end{cases} \tag{2}$$

Supposing that the time-series X is random, independent, and approximately normally distributed, the variance value $\text{Var}(S_k)$ and mean value $E(S_k)$ of statistical variable S_k can be defined as follows:

$$\text{Var}(S_k) = \frac{k(k-1)(2k+5)}{72} \tag{3}$$

$$E(S_k) = \frac{k(k-1)}{4} \tag{4}$$

Then, the statistical sequence UF_k , calculated by the time series X , can be defined as:

$$UF_k = \frac{S_k - E(S_k)}{\sqrt{\text{Var}(S_k)}}, k = 1, 2, \dots, n \tag{5}$$

When the time series X is arranged in reverse order $\{x_n, x_{n-1}, \dots, x_1\}$, then the statistics sequence UF_k can be calculated again using formula (5). By letting $UB_k = -UF_k, (k = n, n-1, \dots, 1)$, then $UB_1 = 0$ to obtain the UB_k statistics sequence. The statistical series of UF_k and UB_k were

graphed in the same coordinates, and the intersection of the two curves was the time of sample mutation. The sample size $n = 62$, and the significance level is $\alpha = 0.05$ (the significance level range is -1.96 to 1.96). The sample series shows an increasing trend when $UF_k > 0$, and a decreasing trend when $UF_k < 0$. If $|UF_k|$ is larger than the significance level, then the series has a significant variation trend.

According to the Chinese classification standards for cold (GB/T 33675-2017) and warm (GB/T 21983-2020) winters, the cold and warm winter classification from 1998 to 2021 was used to define the typical flood prone branches of the Toudaoguai reaches of the river. Table 1 shows the threshold values for cold and warm winter classification. Each winter clustering was further classified as either strong or weak in terms of the temperature, based on the classification standards.

The climatological normal \bar{T} and standard deviation of the average air temperature σ in winter are calculated as follows:

$$\bar{T} = \frac{1}{30} \sum_{i=1}^{30} T_i \quad (6)$$

$$\sigma = \sqrt{\frac{1}{30-1} \sum_{i=1}^{30} (T_i - \bar{T})^2} \quad (7)$$

The average air temperature anomaly in winter of a certain year ΔT is calculated as follows:

$$\Delta T = t - \bar{T} \quad (8)$$

in which T_i and t [$^{\circ}\text{C}$] represent the annual average winter temperature of the target year (previous 30 years) and average temperature of the winter of a certain year, respectively. In this study, the climatological normal \bar{T} updated every decade.

4. Results and discussion

4.1. Temperature change and warm/cold winter classification from 1959 to 2021

Fig. 2 displays the results of the M-K test for the cumulative negative air temperature from 1959 to 2021 at Toudaoguai Hydrological Station. The sample mutation occurred at the crossover point of UF statistics curve (solid red line) and UB statistics curve (blue dotted line). It shows that, over the 62-year period, the Toudaoguai reach experienced a climate mutation (a sharp change in air temperature from one average to another) during the winter flood season of 1987/1988. The value of the UF statistic was greater than 0 from 1974/1975 onwards, indicating that the cumulative negative air temperature in Toudaoguai had a warming trend from 1974/1975 to 2020/2021. The statistical value far exceeds the significance level of $U_{0.05} = 1.96$, especially after 1991/1992, indicating that the warming trend is significant. Since 1991, the winter temperature at Toudaoguai Hydrological Station has shown a significant warming trend, which has an important impact on the ice conditions of the Yellow River.

Fig. 3 shows the classification of winters along the Toudaoguai reach of the main river channel for the period 1998–2021. The threshold values for winter types are calculated every decade, but for the decades

2001–2010 and 2011–2020 the same thresholds apply. In total, seven strong warm winters, five weak warm winters, four normal winters, and seven weak cold winters were reported. The percentages of warm, normal, and cold winters were 52.2%, 17.4%, and 30.4%, respectively. This indicates that, generally, rising air temperature lead to more frequent warm winters. Furthermore, ice-related flooding was mainly observed in cold winters because of extreme weather. For example, in March 2008, the ice jam in the Sanhu Estuary at the Urad Front Banner collapsed, causing a direct economic loss of 69 million CNY. On November 26th, 2015, grounded ice caused flooding over 56.1 km from the dam at the Kuwei River Reach in Wanjiashai, damaging irrigation systems, water engineering works, and the transportation network (Su, 2000; Zhao, 2019; Fang et al., 2009).

4.2. Ice conditions in warm and cold winter years between 1998 and 2021

Temperature changes in winter directly affect the river ice characteristics. This is reflected in the different formation times of ice floods, locations of the cover edge along the river course, channel water storage increments, and low discharge process duration. Table 2 lists the ice characteristics of the Toudaoguai reach and the locations of the initial leading edge of the cover along the Inner Mongolia reach from 1998 to 2021. The average date of the first drift ice (frazil ice first appear) along the reach was November 23, the average date of freeze-up was December 13th, the average date of ice breakup was March 14th, and the average multi-year duration of ice was approximately 112 days. In warm winter years, river freeze-up occurred later, as opposed to the multi-year averages and breakups which commenced at an earlier stage compared with normal and cold winters. The opposite trend was observed for the cold winter years.

The location of the initial leading edge of the cover in the channel is affected by many factors, including air temperature, river topography, hydraulic conditions, and human activities. A comparative analysis of the locations of the initial leading edges of the cover in different years suggests that they were mainly concentrated near Baotou City in warm winters, while in cold winters they were mostly located near Toudaoguai Hydrological Station and Wanjiashai Reservoir. The locations of the initial leading edges of the cover in cold winters moved downstream. This is where the river course flow through canyons, which can easily cause ice jams during the frozen period.

The proportion of mechanical breakups was 52.2 %, whereas that of thermal breakups was 47.8 %. Mechanical breakups occur during years with cold winters, whereas most thermal breakups (72.7%) occur during years with normal or warm winters during which higher air temperatures facilitated ice melting. However, the risk of mechanical breakup was higher in cold winter years.

4.3. Hydraulic condition characteristics in warm and cold winter years between 1998 and 2021

Significant changes in the water flow occur after the river freezes in winter. The existence of an ice cover increases the wetted perimeter of the flow cross-section in the frozen reach and affects the distribution of the flow velocity. Frazil ice continues to flow under the cover, while the buoyancy of larger particles keeps them flowing towards the cover. Greater friction between the ice cover and the flowing frazil ice than that produced by the water drag force causes the ice particles to accumulate on the underside of the cover. According to the critical velocity concept, frazil ice transported from upstream deposits at a cross section until the average flow velocity of the cross section reaches some critical velocity. These may lead to the formation of a hanging dam. The term hanging dam has sometimes been used as a synonym of frazil jam, even though a hanging dam can be formed by accumulations of either surface ice or frazil ice, or combination of both (Shen and Wang, 1995). A large amount of ice is then converted into stored channel water along the

Table 1

Classification of cold and warm winters based on GB/T 33675-2017 and GB/T 21983-2020 standards.

| Grade name | Grade index and threshold |
|--------------------|---|
| Strong warm winter | $\Delta T \geq 1.29\sigma$ |
| Weak warm winter | $0.43\sigma \leq \Delta T < 1.29\sigma$ |
| Normal winter | $-0.43\sigma < \Delta T < 0.43\sigma$ |
| Weak cold winter | $-1.29\sigma < \Delta T \leq -0.43\sigma$ |
| Strong cold winter | $\Delta T \leq -1.29\sigma$ |

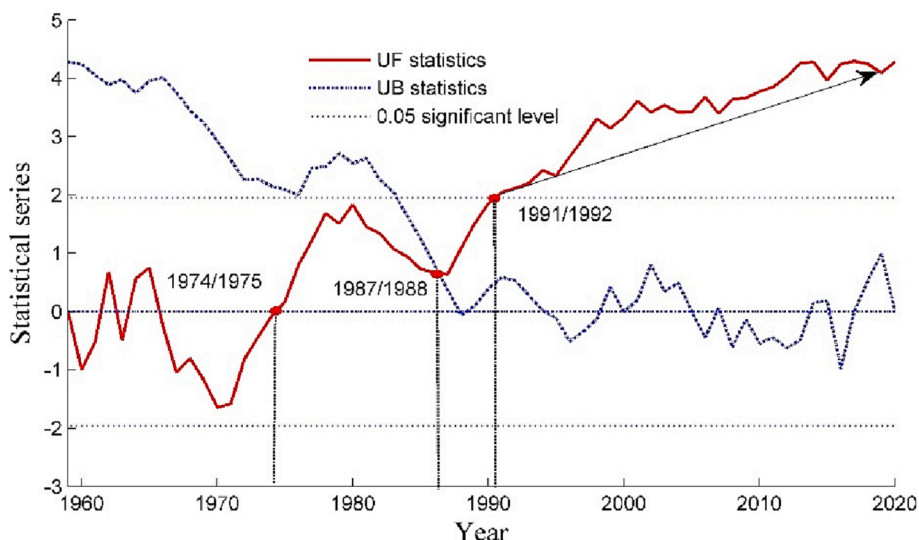


Fig. 2. M-K test results for the cumulative negative air temperature from 1959 to 2021 at Toudaoguai Hydrological Station. Plotted points represent the cumulative negative air temperature from November 1 of the first year to March 31 of the second year of each winter season. 1987/1988 is the mutation year.

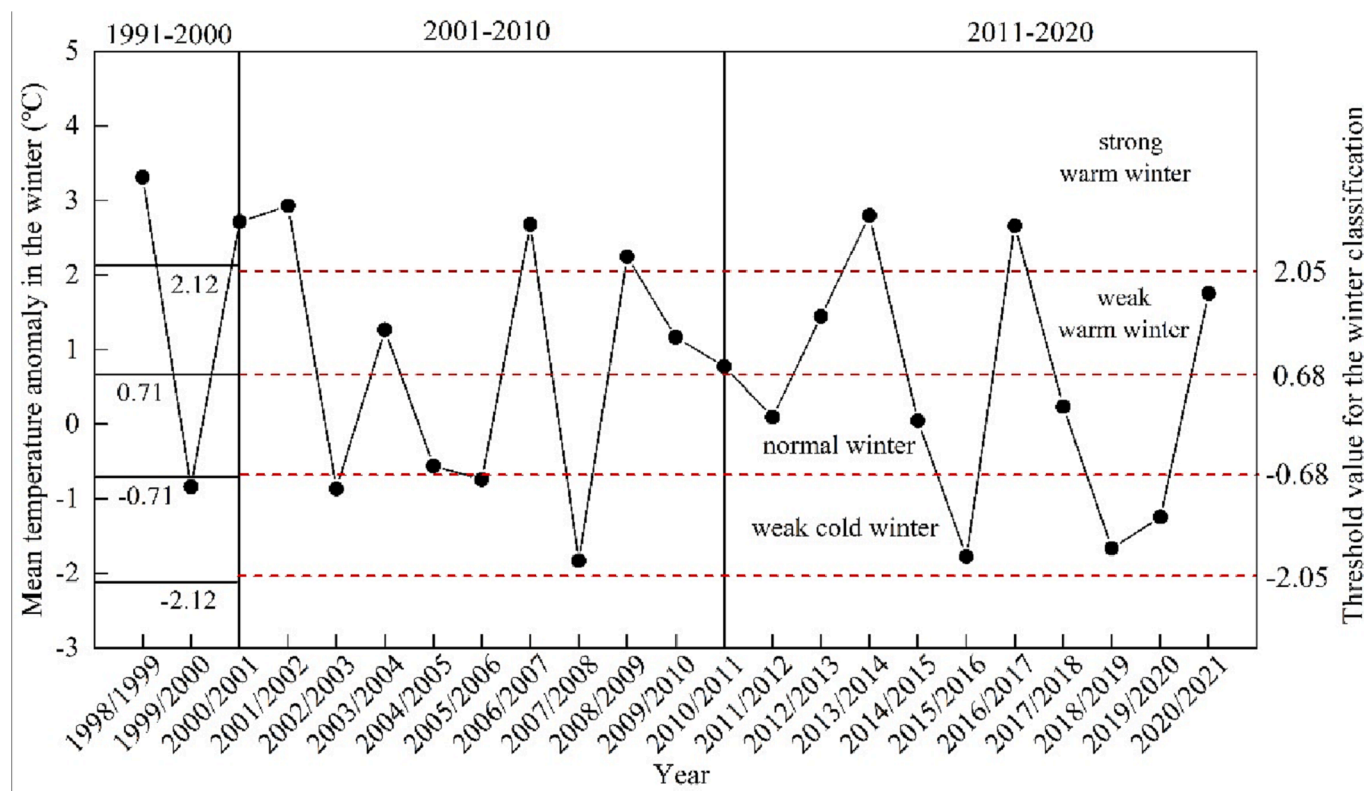


Fig. 3. Classification of winters in the Yellow River from 1998/1999 to 2020/2021 meteorological data collected at Toudaoguai Hydrological Station. (For interpretation of the references to colour in this figure legend, the reader is referred to the web version of this article.)

river, advancing a low discharge process downstream (Prowse and Beltaos, 2002). The longer the duration of this condition, the greater the water and ice storage capacity in the upstream channel. During breakup, large amounts of stored ice and water may be released, leading to a surge in the water level. This increases the risk of a mechanical breakup (Ettema, 2002).

The number of days in which the river had a low-flow in winter from 1998 to 2021 at the Toudaoguai Hydrological Station and the incremental change process for water storage along the Shizuishan-Toudaoguai reach is shown in Fig. 4. The number of consecutive days

characterized by a low-flow and incremental changes in water storage in the channel at the Toudaoguai Hydrological Station show a decreasing trend, with fluctuations, in a warmer climate. Cold winters, with lower cumulative negative temperatures, were more likely to cause extended low-flow duration. In warm winters, freeze-up occurred at a later stage and the ice thickness was relatively thin. As a result, a shorter low-flow period was observed during the ice season. Needless to say, a large water storage amount in line with ice formation along the water course can increase the risk of ice-related flooding during the breakup period.

Table 2

Characteristics of the ice conditions (freeze-up/breakup date, duration, location, and breakup type) along the Inner Mongolian reaches of the Yellow River from 1998 to 2021.

| Year | Ice condition (Month-Day) | | | Duration (days) | | | Location of the initial leading edge of the cover | Breakup type |
|--------------------------------|---------------------------|----------------------|----------------------|-------------------------------|---------------------|---------------------------|--|--------------|
| | First drift ice (1) | Freeze-up (2) | Breakup (3) | Duration of drift ice (2)-(1) | Frozen days (3)-(2) | Duration with ice (3)-(1) | | |
| 1998–1999 (strong warm winter) | Nov 19th | Jan 11th | Mar 4th | 53 | 52 | 105 | Nanhaizi (countryside of Baotou City) | Mechanical |
| 1999–2000 (weak cold winter) | Nov 26th | Dec 9th | Mar 24th | 13 | 105 | 118 | 2 km upstream of Toudaoguai Hydrological Station | Thermal |
| 2000–2001 (strong warm winter) | Nov 12th | Dec 25th | Mar 18th | 43 | 83 | 126 | Under Baotou Railway Bridge | Mechanical |
| 2001–2002 (strong warm winter) | Nov 26th | Dec 13 th | Mar 6th | 17 | 83 | 100 | 25 km downstream of Stirrupkou Yangshui Station in Baotou City | Thermal |
| 2002–2003 (weak cold winter) | Nov 17th | Dec 15th | Mar 22 nd | 28 | 97 | 125 | Lihu Village Reach of Urad Front Banner | Thermal |
| 2003–2004 (weak warm winter) | Nov 22 nd | Dec 13th | Mar 14th | 21 | 91 | 112 | Minjibu in Tuyou Banner of Baotou City | Mechanical |
| 2004–2005 (normal winter) | Nov 25th | Dec 28th | Mar 19th | 33 | 81 | 114 | Nanhaizi Reach in Baotou City | Mechanical |
| 2005–2006 (weak cold winter) | Nov 3 rd | Dec 5th | Mar 16th | 32 | 101 | 133 | Wuqinniu Reach in Baotou City | Mechanical |
| 2006–2007 (strong warm winter) | Dec 1 st | Dec 16th | Mar 16th | 15 | 90 | 105 | Sannyincai in Jiuyuan District of Baotou City | Mechanical |
| 2007–2008 (weak cold winter) | Nov 27th | Dec 13th | Mar 14th | 16 | 91 | 107 | Caojiawan Reach, Qingshuihe County, Hohhot City | Mechanical |
| 2008–2009 (strong warm winter) | Nov 26th | Dec 23 rd | Mar 2 nd | 27 | 69 | 96 | 4 km upstream of Sanhu Estuary Section | Mechanical |
| 2009–2010 (weak warm winter) | Nov 15th | Dec 9th | Mar 24th | 24 | 105 | 129 | Dengkou Reach of Donghe District in Baotou City | Mechanical |
| 2010–2011 (weak warm winter) | Nov 25th | Dec 13th | Mar 19th | 18 | 96 | 114 | 21 km downstream of Fengzhunn Railway Bridge | Thermal |
| 2011–2012 (normal winter) | Dec 4th | Dec 19th | Mar 20th | 15 | 91 | 106 | 500 m from Dengkou in Baotou City | Thermal |
| 2012–2013 (weak warm winter) | Nov 16th | Dec 1 st | Mar 8th | 15 | 97 | 112 | Baotou Baoshen Railway | Mechanical |
| 2013–2014 (strong warm winter) | Nov 27th | Dec 15th | Mar 18th | 18 | 93 | 111 | 4 km from Toudaoguai Hydrological Station | Mechanical |
| 2014–2015 (normal winter) | Nov 30th | Dec 7th | Mar 18th | 7 | 101 | 108 | Zhaojun Tomb, Jiuyuan District, Baotou City | Thermal |
| 2015–2016 (weak cold winter) | Nov 27th | Dec 15th | Mar 18th | 18 | 93 | 111 | 6 km from Toudaoguai Hydrological Station | Thermal |
| 2016–2017 (strong warm winter) | Nov 21 st | Nov 29 th | Mar 16th | 8 | 107 | 115 | Sanhu Estuary Hydrological Station | Thermal |
| 2017–2018 (normal winter) | Nov 18th | Dec 4th | Mar 15th | 16 | 101 | 117 | Shishizi, 4 km from Toudaoguai section | Thermal |
| 2018–2019 (weak cold winter) | Dec 4th | Dec 11th | Mar 22 nd | 7 | 101 | 108 | 1 km on Sanhu Estuary | Mechanical |
| 2019–2020 (weak cold winter) | Nov 25th | Dec 6th | Mar 14th | 11 | 98 | 109 | Shisifenzi Reach | Thermal |
| 2020–2021 (weak warm winter) | Nov 24th | Dec 14th | Mar 10th | 20 | 86 | 106 | 17 km from Baotou Hydrological Station | Thermal |
| Average date | Nov 23 rd | Dec 13th | Mar 14th | 21 | 92 | 112 | | |
| Years with strong warm winters | Nov 22 nd | Dec 16th | Mar 10th | 26 | 82 | 108 | | |
| Years with weak warm winters | Nov 24th | Dec 10th | Mar 18th | 20 | 95 | 115 | | |
| Years with cold winters | Nov 28th | Dec 12th | Mar 19th | 18 | 98 | 116 | | |
| Normal winters | Nov 17th | Dec 13th | Mar 17th | 18 | 94 | 111 | | |

Notes: the dates of first drift ice, freeze-up, and breakup refer to the date when the frazil ice, ice cover, and ice melting first appear in the river, respectively.

4.4. Runoff characteristics and sediment transport changes in warm and cold winter years between 1998 and 2021

Runoff and sediment transport data were collected at Toudaoguai Hydrological Station during each winter season to determine the correlation between these two variables and their variation between warm and cold winters. The sediment concentration under ice-cover flow is fairly low compared to that in summer, but for the same cumulative percentage undersize, the median grain size of suspended load under ice cover is much coarser than that under open flow conditions (Sui et al., 2005). Fig. 5 shows that runoff during the ice flood season had a significant positive correlation of quadratic function with the amount of

transported sediment ($p < 0.05$; Pearson correlation). The maximum and minimum runoff values along the river reach occurred in 2020/2021 (a weak warm winter) and 2002/2003 (a weak cold winter), respectively. However, the maximum and minimum sediment transport amounts occurred in 2007/2008 (a weak cold winter) and 2016/2017 (a strong warm winter), respectively. Although there was a positive correlation between runoff and sediment transport during the ice flood season, these parameters were affected by the climate characteristics and ice conditions during both cold and warm winters. It should be noted that the inter-annual maximum runoff in winter did not necessarily correspond to the maximum amount of transported sediment. The largest amount of runoff and sediment transport was observed in cold

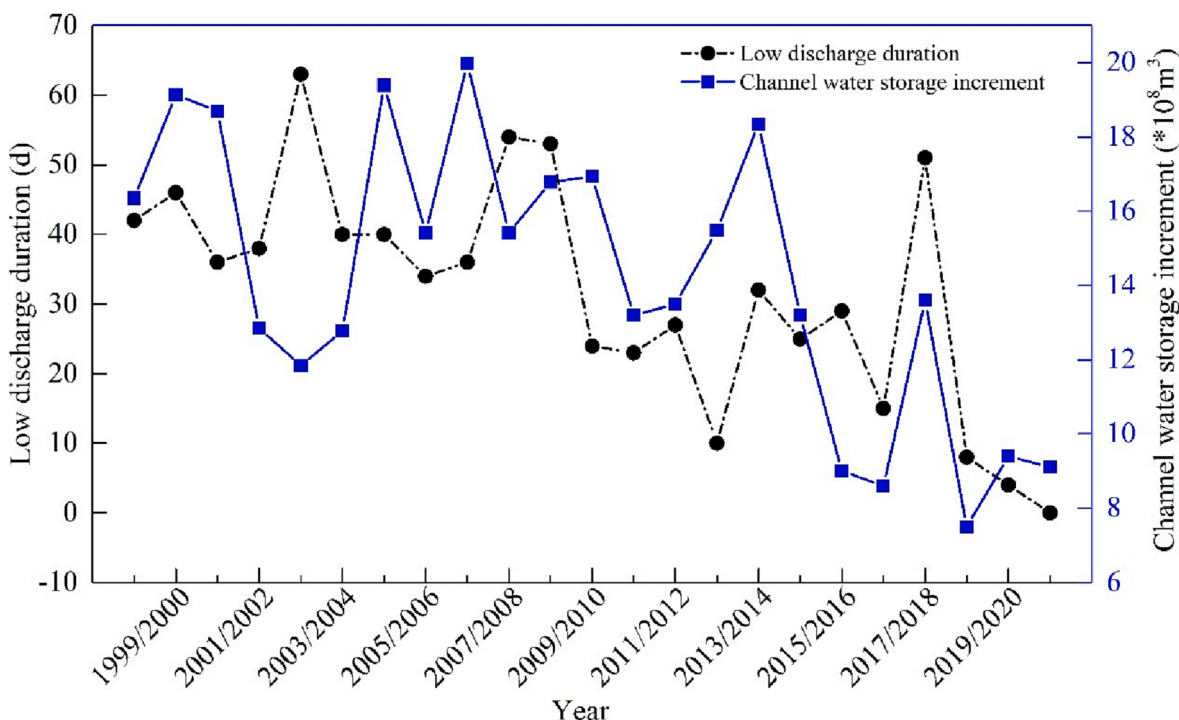


Fig. 4. Characteristics of the low discharge duration (warm winter: 29 d, normal winter: 36 d, weak cold winter: 34 d) in the Toudaoguai reach of the Yellow River and changes in channel water storage increment (warm winter: $14.92 \times 10^8 \text{ m}^3$, normal winter: $14.92 \times 10^8 \text{ m}^3$, weak cold winter: $12.53 \times 10^8 \text{ m}^3$) in the Inner Mongolia reaches of the Yellow River during the ice period. (For interpretation of the references to colour in this figure legend, the reader is referred to the web version of this article.)

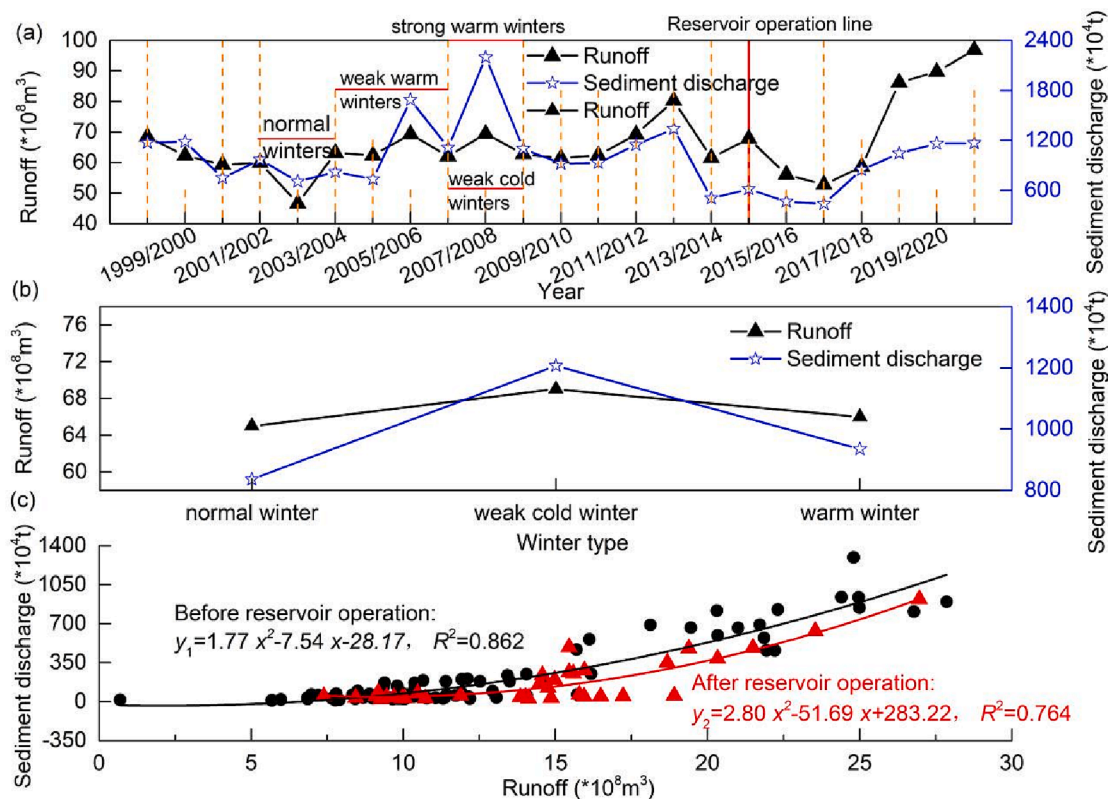


Fig. 5. Variations in runoff and sediment transport along the Toudaoguai reach of the Yellow River from 1998 to 2021. (a) Runoff and sediment transport amounts in different years; (b) variations in runoff and sediment transport among different winter types; (c) Pearson correlation analysis between runoff and sediment transport during the winter season before and after the Haibowan reservoir operation. (For interpretation of the references to colour in this figure legend, the reader is referred to the web version of this article.)

winters, as shown in Fig. 5(b). Among the other two types of winter, runoff and sediment transport amounts do not vary much, but are slightly higher in warm winters than in the normal winters. Fig. 5(c) shows that the effect of reservoir is evident in changing the correlation between runoff and sediment load. Generally, the existence of the reservoir reduces sediment load. Based on Fig. 5(a), during construction and operation of the reservoir (from 2014/2015), the lines related to runoff and sediment discharge start to get distance. In other words, it can be seen that water flow transports less sediment during the winter season.

Substantial runoff and sediment transport in cold winters may lead to a higher risk of scouring and silting in the channel. These phenomena, along with ice emergence, transport, and jamming lead to channel evolution and ice-related flooding during the ice flood season. There was relatively low runoff and transportation during the warm winter seasons. However, the mismatch between runoff and sediment transport during warm winters increased the possibility of a high flow and low sediment content or a low-flow and high sediment content during warm winters, resulting in scouring and silting along the river course.

An overall positive correlation between the channel water storage increment and low-flow process corresponding to the difference between cold and warm winters is observed. This correlation is complex due to the meteorological condition that characterizes the winter season and the hydraulic as well as morphological features of the river. The increase in water storage in the channel during ice period (November 1 to March 31) was calculated based on data obtained from stations that cover the entire Inner Mongolian reach of the Yellow River (between Shizuishan and Toudaoguai hydrological stations; Fig. 1). The water head loss and extent of the frozen reaches have increased uncertainty in relation to the changes in channel water storage. Although the correlation between the channel water storage increment and low-flow duration at the Toudaoguai Hydrological Station from 1998 to 2021 was significant ($p < 0.05$; two-tailed Pearson correlation), the channel storage increment corresponding to the extended low-flow period in cold winters was not as large as that during warm winters.

The frazil jam profile is primarily determined by the flow's ice

transport capacity, with the freezing effect also playing a possible role (Shen and Wang, 1995). Under the condition of ice jam, the flow is affected by the roughness of ice jam, the roughness of riverbed and the seepage resistance through ice rubble, which leads to increases in the water level and stored water amount (Fan et al., 2019; Zhao and Shen, 2021). Consequently, except for the jam toe area, there is generally a lower rate of sediment yielding and greater sediment deposition in the winter season. Under the jam toe, due to the reduced inlet area of the flow and the increase in water velocity, the shear tension on the bed level rises, increasing the drag force on the bed materials. Hence, bed erosion in this section can be expected (Knack and Shen, 2017). Sediment is then transported downstream with higher discharge and turbulence.

Three typical years, i.e., 2007/2008 (a weak cold winter), 2011/2012 (normal winter), and 2013/2014 (a strong warm winter), were selected to analyze the changes in the average daily sediment content of the channel during the ice flood season, as shown in Fig. 6.

The average sediment content of the water flow indicates an increasing-decreasing-increasing tendency during the ice flood season (Fig. 6). For the weak cold winter the sediment concentration rate for freeze-up period reached up to 6 kg/m^3 and around 12 kg/m^3 for breakup. For the other two winter types – normal and strong warm, the sediment concentration during the freeze-up was in the range of $1\text{--}2 \text{ kg/m}^3$. For breakup the strong warm winter shown lower sediment concentration (4 kg/m^3) in comparison to the normal winter (8 kg/m^3). Before the river was frozen, the runoff variation significantly affected the average sediment content along the river course, which is largest and smallest during cold winters and strong warm winters, respectively. The river's runoff significantly decreased after freezing, ranging from 30% to almost 70% of the discharge prior to freeze-up, depending on the type of winter. A gradual decrease in air temperature enhance the increase in ice layer thickness. The increased roughness of the bottom of the ice mass and riverbed resistance caused decreased conveyance of the channel, which in turn resulted in less flow energy available to transport sediment. While the cover was present, the sediment content reached the lowest level and stabilized. After river breakup, the inflow of water from

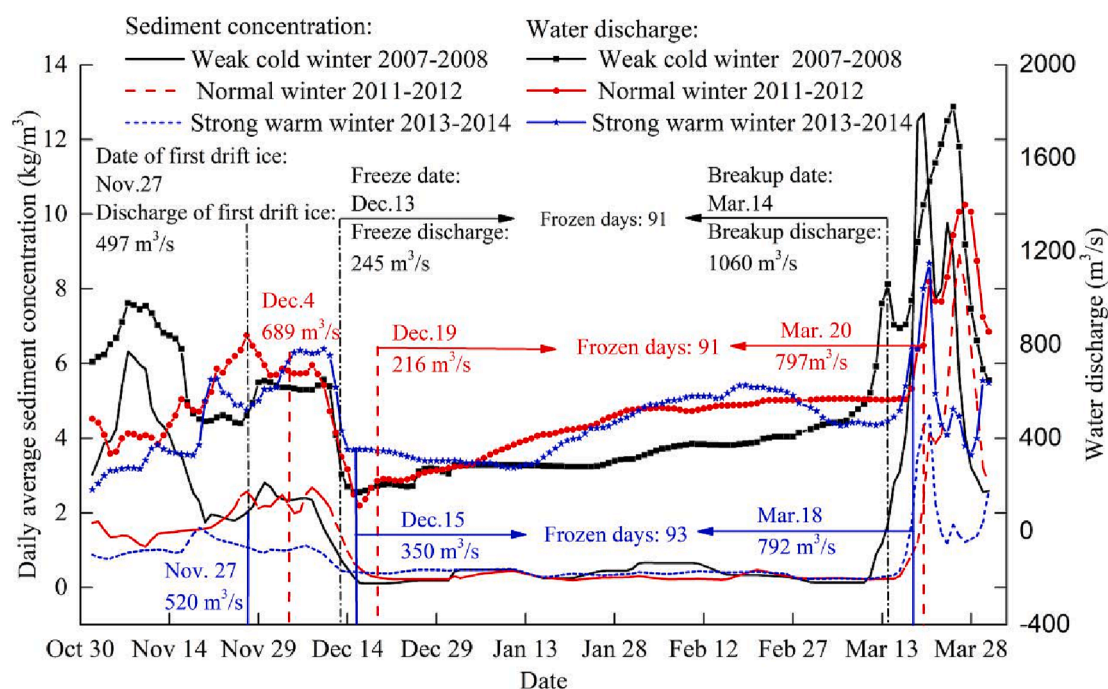


Fig. 6. Variations in the average daily sediment content in a typical year along the Toudaoguai reach of the Yellow River in Inner Mongolia (the black lines represents the weak cold winter from 2007 to 2008; the red and blue lines represent the normal winter 2011/2012 and strong warm winter 2013/2014, respectively). (For interpretation of the references to colour in this figure legend, the reader is referred to the web version of this article.)

the upper reaches, which was previously stored as the ice jams, increased. Therefore, there was a significant increase in the sediment content in the water flow and ice mass. In addition, sediment may have become discharged into the water course due to riverbank collapse, with the maximum amount reaching 5–10-fold that of the freeze-up period. In the winters of 2007/2008 (a weak cold winter), 2011/2012 (a normal winter), and 2013/2014 (a strong warm winter), the flow differences between the freeze-up and breakup periods were 815, 350, and 442 m³/s, respectively. A rapid increase in the flow and changes in the sediment content during the breakup period of the cold winters far exceeded that of the warm winters. Complex ice regime characteristics extended the period of low-flow, and considerable water discharge into the river course aggravated the problems associated with flood control along the river channel during the ice flood season in cold winters. In warm winter years, the unique runoff and sediment change characteristics during the flood period also increased the difficulty associated with examining the evolution of riverbed scouring and silting, as well as the risk of a “secondary suspended river” developing.

The sediment concentration during the frozen period was 5–20-fold smaller than that in the open water period while the amount of transported sediment was 2–15-fold smaller. Potential spots for the formation of border ice include shallower and less turbulent areas, where coarse-grained sediments tend to deposit. During ice breakup, the stored water under the ice cover is released, increasing the water discharge rate. As a result, more sediment is carried with the flow. The bed section where the breakup occurs undergoes scouring and erosion. The amount and process of the sediment transport during the breakup period may vary according to changes in ice type. The data analyzed in this study suggest that the stronger the winter seasons become, the weaker the correlation between water discharge and sediment transport rates is observed.

4.5. Relationship between the suspended sediment transport rate and the discharge rate between 1998 and 2021 according to winter type

The suspended sediment transport rate may vary in different ice-related flow conditions, i.e., in open water, freeze-up, ice cover, and breakup conditions. A schematic diagram of the periods of these conditions is shown in Fig. 7. Fig. 8 shows the suspended sediment load associated with different discharges into open water before the freeze-up period (November 1 to the commencement of the first drift). Divide this period into four periods on average, each period as one quarter. The size of the dots indicates the variation from the first to the last dates in the period. Larger dots indicate the dates closer to the first ice drift. The nonlinear correlation between these parameters is related to the varying phase of the water condition due to following ice drift, and more concentrated data set at the adjacent of freeze-up date. A weak linear correlation between sediment transport rate and water discharge rates can be observed for the whole dataset, although a stronger linear correlation is found for the dates far from the freeze-up condition. Moreover, the rate of the sediment transport generally decreases as the freeze-up period approaches, which may be attributed to the trapped sediment particles in frazil ice. For the dates farthest from the first ice drift, the

sediment transport rates related to the discharges higher than 800 m³/s comprise the highest values.

Fig. 9 shows the suspended sediment transport rate in relation to the discharge during the freeze-up period (first drift to the commencement of the freeze-up). Lower discharge values are observed for the days that are closest to the period in which the ice cover was formed. This may have resulted from the increase in the water level, which caused a reduction in the suspended sediment transport rate. Lower transport rates of suspended sediment may be related to the ice cover thickness, velocity distribution, and shear stress. Based on Fig. 9, the further the date is from cover formation, the more scattered is the relationship between the sediment transport rate and the discharge rate, causing the nonlinear correlation that can be observed across the entire data set.

Fig. 10 shows the suspended sediment transport rate during ice cover. For discharge rates less than 650 m³/s (the related discharge rate for ice cover expansion prior to breakup), straight line sets of data can be distinguished, implying a roughly unified sediment transport rate despite the large variation in the discharge rate. This may be due to the existing cover resistance, which leads to an increased water level and less shear tension on the river bed. The large increases in the sediment transport rate despite no significant changes in the rate of discharge may be due to the local features of the cover, i.e., undercover ice accumulation and cover meeting sharp ice jam toe formation. The mentioned occurrences may cause a decrease in the flow transaction area, which leads to bed erosion and the resultant sediment transport rate (Kolerski and Shen, 2015). Furthermore, they may be related to bank scouring and bank collapse due to ice cover movement in specific spots. One example of the rough changes in this reach is the evolution of the Shensifenzi bend area from 1995 to 2013 (Zhao et al., 2021).

In Fig. 11, different discharge and sediment transport rates related to the breakup type and winter type as well as the date of breakup are presented, which discharge and suspended sediment data are the data of the day when the ice cover firstly melt. No specific trend for winter type can be seen from the plot. This suggests that there are other parameters influencing the relationship between discharge and sediment transport rates other than hydrometeorological conditions. Additionally, a higher sediment transport rate in the breakup period is observed in comparison with the freeze-up and ice cover period, it also can be inferred that on the first day of breakup, the sediment transport condition is mostly influenced by the existing broken cover.

In Fig. 12, the open water condition after breakup for different winter types is presented. A weak correlation can be observed between the suspended sediment transport rate and the discharge rate for different winter types, resulting from large variation in one parameter versus minor changes in the other. This trend also can be attributed to the uncertainty of the flow condition on account of the ice run and jam after the breakup. Furthermore, it may be related to the sediment pulse and peak of the jam-generated waves, which may not necessarily coincide as a result of local erosion in heavy runs (Beltaos, 2016). The breakup event typically has large concentrations of suspended sediment, and the suspended sediment rate in the post-breakup can reach three times that of the open water period, which causes a large portion of the annual sediment load occurs during the breakup period.

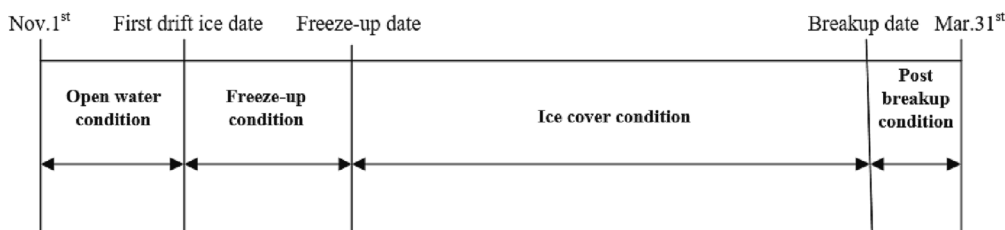


Fig. 7. Schematic diagram of the periods of open water (duration from Nov 1 to the first drift ice date), freeze-up (duration from the first drift ice date to the freeze-up date), ice cover (duration from the freeze-up date to the break up date), breakup (breakup date) and post breakup (duration from the breakup date to Mar 31) conditions.

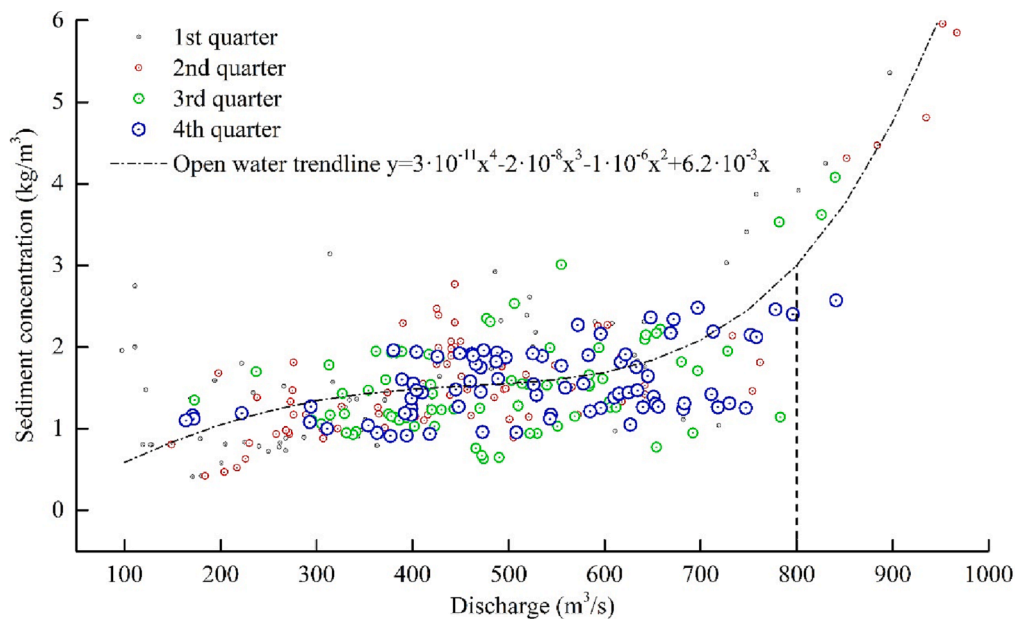


Fig. 8. Relationship between the suspended sediment transport rate and discharge rate during open water condition (the period from November 1 to the first drift ice date, divide this period into four equal periods, each period as one quarter, the smaller the dots, the closer it is to November 1).

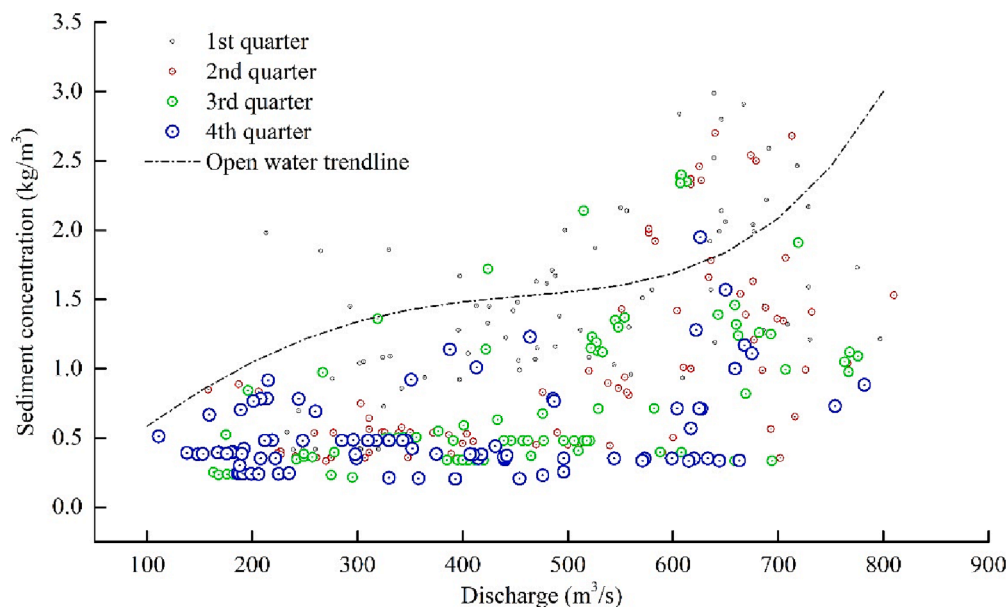


Fig. 9. Relationship between the suspended sediment transport rate and discharge rate during freeze-up condition (the period from first drift to the freeze-up date, divide this period into four equal periods, each period as one quarter, the smaller the dots, the closer it is to the first drift ice date).

Overall, the suspended sediment transport rate in the open water condition and post breakup condition shows higher values which is mostly observed in post breakup condition. This increased rate can be observed during the ice cover period for the days in which breakup is anticipated in comparison to the dates on which the ice cover is present.

In summary, there is a complex relationship among hydrodynamic conditions, channel morphology, the sediment transport rate, and ice dynamics, through which the meteorological condition (winter type) and type of breakup affect sediment transport in the channel. Further studies on this phenomena in various winter types is recommended.

5. Conclusions

In recent decades, the increase in water storage has shown a

declining trend (as indicated by the low-flow process) in the Inner Mongolia reaches of the Yellow River. This could be attributed to sediment deposition on the riverbed, global warming, and extreme weather events, as well as anthropogenic causes including engineering works and reservoir operations. Therefore, the mechanism of interaction among hydrodynamic conditions, meteorological conditions, and the sediment transport rate, taking into account the impact of climatic changes on these regions, requires further investigation. To address this objective, this study analyzed data related to these factors, which were collected from hydrological stations during different types of winter seasons from 1959 to 2021. The multi-year mean water discharge was $589 \text{ m}^3/\text{s}$, and the average multi-year temperature was $9 \text{ }^\circ\text{C}$. The mutation year under climate change was calculated (the winter season of 1987/1988), and the winters were classified based on the cumulative negative air

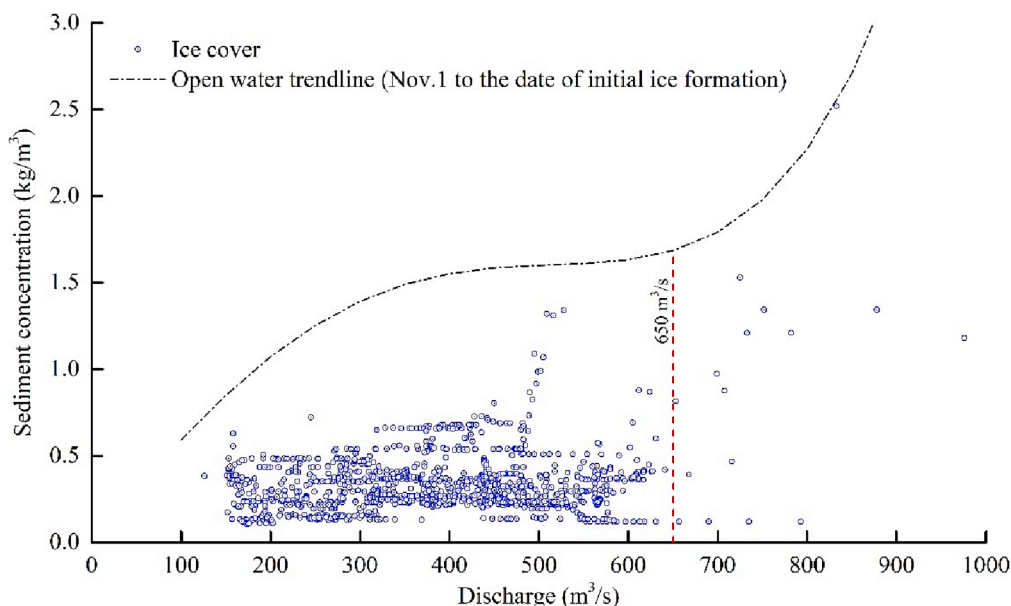


Fig. 10. Relationship between the suspended sediment transport rate and discharge rate during ice cover condition (the period from freeze-up date to the breakup date).

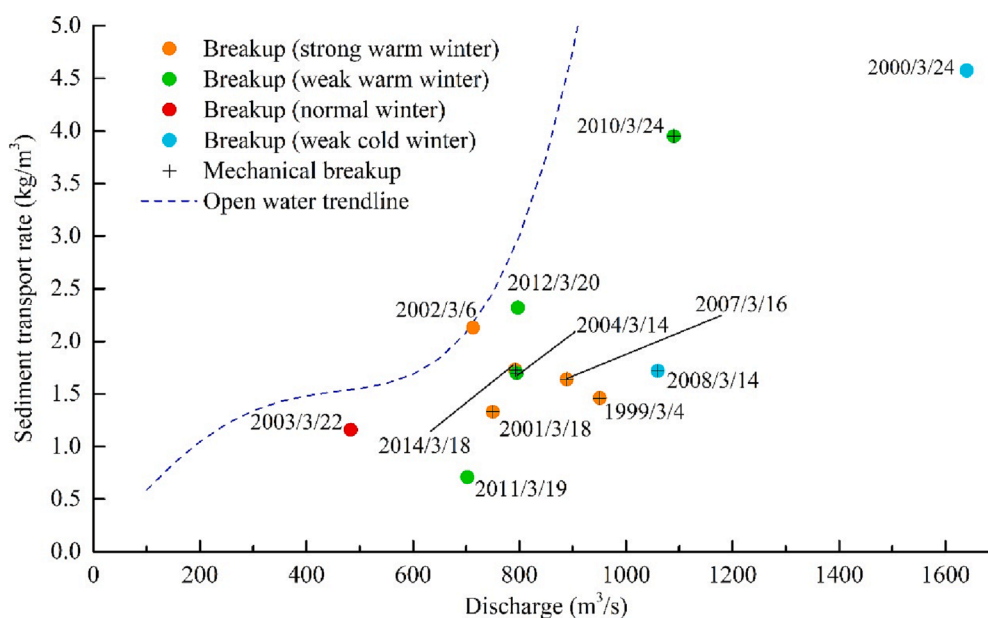


Fig. 11. Relationship between the suspended sediment transport rate and the discharge rate during breakup condition of different winter types (the breakup date).

temperature and the M-K mutation test. Seven, five, four and seven winters were recoded as strong warm, weak warm, normal and weak cold winters, respectively. The study reveals the characteristics of ice, water, sediment and their interaction mechanism in cold and warm winters, providing a theoretical basis for the regulation of ice and rational allocation of water resources.

The results indicate a clear upward trend in temperature since 1988. The climate mutation demonstrates the severe effect of the warming trend over the study period ($UF > 0$). Based on the clustering system for winter types (cold and warm), warm winters dominated, occurring three times as often as cold winters (with percentages of occurrence for warm, normal, and cold winters being 52.2%, 17.4%, and 30.4%, respectively). As a result, ice-related flooding was observed in one quarter of all winters studied. Analysis of climate-related ice phenomena, revealed the changes may cause tardy freeze-ups, preceding multi-year averages, and

breakups. Moreover, the location of the initial edge of the cover moved further downstream (mainly appearing near Baotou City in warm winters, while moving downstream to Toudaoguai Hydrological Station and Wanjiashai Reservoir in cold winters). The analysis of the data related to low-flow and water storage increase suggests a declining trend in both parameters in warm winters, possibly due to the shorter duration of freeze-ups and lower ice thicknesses. Overall, the results suggest that extended low-flow durations in cold winters with less cumulative negative air temperatures are more likely than in warm winters. The Pearson test was employed to examine the sediment transport trend and its relation to runoff, as well as changes in different winter types. Runoff and sediment levels varied with changing climatic and ice conditions in cold and warm winters, and a positive correlation of quadratic function was observed ($p < 0.05$). Reservoir construction and operation further affected the relationship between runoff and sediment transport. The

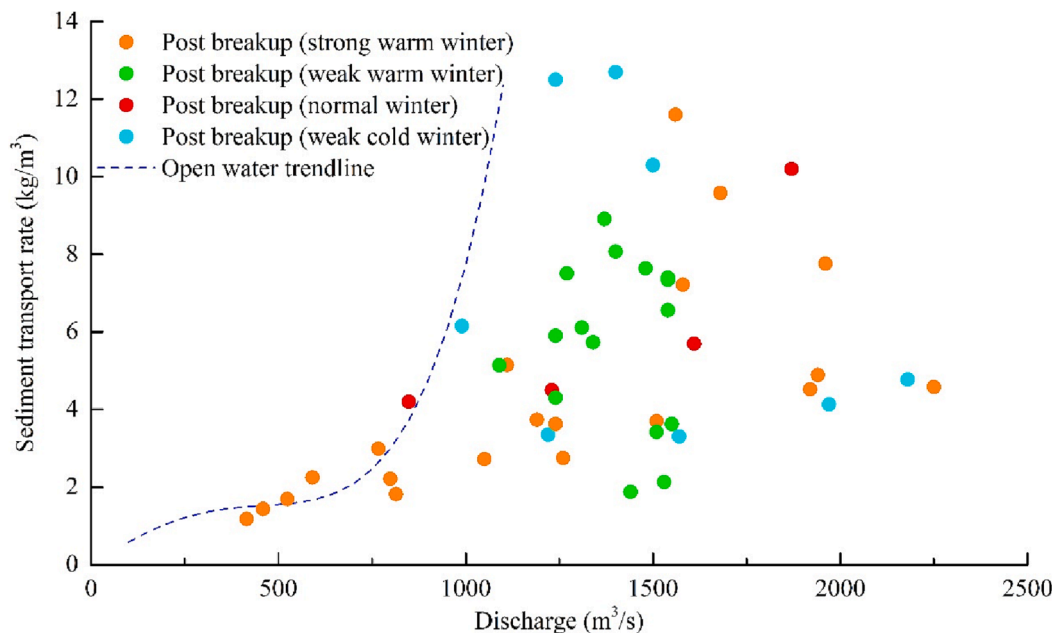


Fig. 12. Relationship between the suspended sediment transport rate and the discharge rate during post-breakup condition of different winter types (the period from breakup date to March 31).

cold and weak warm winters showed a correlation between runoff and sediment transport; the largest and lowest values for these parameters occur during the cold and weak warm winters, respectively. In cold winters, higher runoff and sediment transport led to higher channel evolution that is intensified by ice formation, transport, and jamming. However, during the warm winters, scouring due to high flow, low sediment content, and silting as a result of the low-flow and high sediment content may have led to channel evolution. A significant correlation between low-flow duration and channel water storage increment was observed at Toudaoguai Hydrological Station between 1998 and 2021 ($p < 0.05$), although the correlation was more pronounced during warm winters. Analysis of the typical weak cold and weak warm winters, as well as the strong warm winters, suggests an increasing sediment transport rate during the pre-freeze-up period occurs as a consequence of increased runoff. Because of the increased roughness and weakened vertical turbulent mixing following the freeze-up period, the sediment transport rate decreases, reaching its lowest level during the cover period. After breakup, on account of the increased runoff, high flow, and bank collapse, an increased sediment transport rate is observed. The flow rate and sediment transport after river breakup were increased 3–5 and 5–10 fold, respectively. No strong correlation between runoff and sediment transport was observed during the breakup in cold winters. It can be concluded that the type of ice and its movement in the flow influences the sediment transport rate, rather than the runoff itself. Generally, a non-linear correlation is observed between the suspended sediment transport rate and the discharge rate for the different ice condition periods. The lowest suspended sediment transport rate can be observed during the ice cover and freeze-up periods. It can be suggested that with the exception of the local ice condition, i.e., jamming or the toe section of the ice formation, might reduce the suspended sediment transport rate.

A warmer climate has slightly reduced the necessity for disaster prevention and mitigation. However, more preventive measures are needed in the cold winter years. Furthermore, the uncertainty caused by uncoordinated runoff and sediment processes during warm winters requires specific attention.

CRediT authorship contribution statement

Shuixia Zhao: Conceptualization, Methodology, Writing – original draft, Writing – review & editing. **Quancheng Zhou:** Methodology, Writing – original draft. **Wenjun Wang:** Supervision, Writing – review & editing. **Yingjie Wu:** Data curation, Validation. **Chao Li:** Data curation, Formal analysis. **Qiang Quan:** Validation, Software. **Parisa Radan:** Writing – review & editing. **Youcai Tuo:** Visualization, Investigation. **Tomasz Kolerski:** Validation, Writing – review & editing.

Declaration of Competing Interest

The authors declare that they have no known competing financial interests or personal relationships that could have appeared to influence the work reported in this paper.

Data availability

Data will be made available on request.

Acknowledgments

This research was funded by the Natural Science Foundation of Inner Mongolia Autonomous Region (No. 2020BS05038); the National Natural Science Foundation of China (No. 52009084); the Natural Science Foundation of Inner Mongolia Autonomous Region (Nos. MK0143A012022 and 2021GG0089); the IWHR Research & Development Support Program (Nos. MK0145B022021 and MK2022J09) and the IWHR Internationally-oriented Talents Program.

References

- Beltaos, S., 2016. Extreme sediment pulses during ice breakup, Saint John River, Canada. *Cold Reg. Sci. Technol.* 128, 38–46.
- Beltaos, S., Prowse, T., 2009. River-ice hydrology in a shrinking cryosphere. *Hydrol. Process.* 23 (1), 122–144.
- Chen, W., Lan, X.Q., Wang, L., Ma, Y., 2013. The combined effects of the ENSO and the Arctic Oscillation on the winter climate anomalies in East Asia. *Chin. Sci. Bull.* 58 (12), 1355–1362.
- Decker, H., Leonard, Z., 2004. Laboratory Test of Scour Under Ice: Data and Preliminary Results. US Army Corps of Engineers, America.

- Du, H.L., Xu, Y.P., Hu, B.H., 2014. Effect of temperature on ice flood of the Yellow River. *Meteorol. Hydrol. Marine Instrum.* 31 (04), 29–32 in Chinese.
- Ettema, R., 2002. Review of alluvial-channel responses to river ice. *J. Cold Reg. Eng.* 16 (4), 191–217.
- Ettema, R., 2006. Ice effects on sediment transport in rivers. In: Garcia, M.H. (Ed.), *Sedimentation Engineering*. ASCE Publications, Reston, VA.
- Fan, L., Mao, Z.Y., Shen, H.T., 2019. Hydraulic resistance of river ice jams. *J. Hydrodyn.* 31 (3), 504–511.
- Fang, L., Feng, X.M., Yan, B.W., et al., 2009. Analysis on ice flood damaged dike from the location of the Inner Mongolia Hangjinqi Duguitalakuisu region of the Yellow River. *J. Eng. Heilongjiang Univ.* 36 (01), 31–33 in Chinese.
- Fu, H., Wang, J., Yang, K.L., et al., 2007. Study of sediment transport during freezing period. In: *Proceedings of the Third National Conference on Hydraulics and Hydraulic Informatics*. Chinese Hydraulic Engineering Society, pp. 494–499.
- Gao, G.M., Li, S.X., Zhang, B.S., et al., 2019. Ice jam evolution and riverbed scouring and silting characteristics of the Toudaoguai section of the Yellow River during the flood period of 2013 to 2014. *China Flood Drought Manage.* 29 (2), 20–22 in Chinese.
- He, S., 2013. Reduction of the East Asian winter monsoon interannual variability after the mid-1980s and possible cause. *Chin. Sci. Bull.* 58 (12), 1331–1338.
- Ji, H.L., Liu, Q., Gao, G.M., et al., 2019. Study on the characteristics of extreme low temperature change in winters in the lower Yellow River and its influence on ice regime. *Water Resour. Hydropower Eng.* 50 (11), 25–34 in Chinese.
- Kämäri, M., Alho, P., Veijalainen, N., Aaltonen, J., Huokuna, M., Lotsari, E., 2015. River ice cover influence on sediment transportation at present and under projected hydroclimatic conditions. *Hydrol. Process.* 29 (22), 4738–4755.
- Knack, I., Shen, H.T., 2015. Sediment transport in ice-covered channels. *Int. J. Sedim. Res.* 30 (1), 63–67.
- Knack, I.M., Shen, H.T., 2017. Numerical modeling of ice transport in channels with river restoration structures. *Can. J. Civ. Eng.* 44 (10), 813–819.
- Knack, I., Shen, H.T., 2018. A numerical model for sediment transport and bed change with river ice. *J. Hydraul. Res.* 56 (6), 844–856.
- Kolerski, T., Shen, H.T., 2015. Possible effects of the 1984 St. Clair River ice jam on bed changes. *Can. J. Civ. Eng.* 42 (9), 696–703.
- Paul, A., Bhowmik, R., Chowdhary, V.M., Dutta, D., Sreedhar, U., Sankar, H.R., 2017. Trend analysis of time series rainfall data using robust statistics. *J. Water Clim. Change* 8 (4), 691–700.
- Polvi, L.E., Dietze, M., Lotsari, E., Turowski, J.M., Lind, L., 2020. Seismic monitoring of a subarctic river: seasonal variations in hydraulics, sediment transport and ice dynamics. *J. Geophys. Res. Earth Surf.* 125 (7) <https://doi.org/10.1029/2019JF005333>.
- Prowse, T.D., 2001. River-ice ecology. I. Hydrologic, geomorphic, and water-quality aspects. *J. Cold Reg. Eng.* 15, 1–16.
- Prowse, T.D., Beltaos, S., 2002. Climatic control of river-ice hydrology: a review. *Hydrol. Process.* 16 (4), 805–822.
- Quan, D., Li, C.Y., Li, C., et al., 2018. Study on distribution characteristics of suspended load in the Yellow River. *J. Sedim. Res.* 43 (2), 2–26.
- Ran, D.C., Yao, W.Y., Shen, Z.Z., et al., 2015. Analysis on the contribution rate of driving factors for the annual water and sediment variations at the Toudaoguai hydrological station in the Yellow River. *Adv. Water Sci.* 26 (06), 769–778.
- Shen, H.T., Wang, D.S., 1995. Under cover transport and accumulation of frazil granules. *J. Hydraul. Eng.* 121 (2), 184–195.
- Su, M.L., 2000. Review of the Yellow River ice prevention work in 1999–2000 and analysis of the ice prevention situation in 2000–2001. *Yellow River* 22 (12), 1–2.
- Sui, J., Jackson, P., et al., 2005. Investigations of the sediment budget of a reach of the Yellow River in the Loess Plateau. *IAHS AISH Publ.* 66 (16), 8233–8240.
- Sui, J.Y., Wang, D.S., Bryan, W.K., 2000. Suspended sediment concentration and deformation of riverbed in a frazil jammed reach. *Can. J. Civ. Eng.* 27 (6), 1120–1129.
- Tian, F.C., Yuan, X.M., He, L.X., et al., 2022. Research on characteristics of river regime evolution and its relationship with ice flood disasters in Inner Mongolia reach of the Yellow River (IMYR) based on fractal theory. *J. Hydraul. Eng.* 1–12.
- Turcotte, B., Morse, B., Bergeron, N.E., Roy, A.G., 2011. Sediment transport in ice-affected rivers. *J. Hydrol.* 409 (1–2), 561–577.
- Wang, J., Sun, L.J., 1998. A laboratory study of starting velocity of non-cohesive sediment under ice cover. *Hydro-Sci. Eng.* 02, 164–169.
- Wang, Y., Wu, B., Zhong, D., Wang, Y., 2016. Calculation method for sediment load in flood and non-flood seasons in the Inner Mongolia reach of the Yellow River. *J. Geog. Sci.* 26 (6), 707–721.
- You, Q., Kang, S., Pepin, N., Flügel, W.-A., Sanchez-Lorenzo, A., Yan, Y., Zhang, Y., 2010. Climate warming and associated changes in atmospheric circulation in the eastern and central Tibetan Plateau from a homogenized dataset. *Glob. Planet. Change* 72 (1–2), 11–24.
- Zhang, J.L., Lu, J., 2021. Response mechanism of ice floods to scour and silting evolution in the Inner Mongolian channel and reaches of the Upper Yellow River. *Adv. Water Sci.* 32 (2), 192–200.
- Zhang, Y.J., Yu, J.H., Liu, Z.Y., et al., 2013. Winter 2009/2010 Temperature Anomaly in China and Its Remote Response to Sea Surface Temperature. *Clim. Environ. Res.* 18 (05), 626–638.
- Zhao, S.X., 2019. *Studies on Freeze-Up and Breakup Thermodynamic Simulation and Hydro-Ice Dynamics Mechanism of Ice Jams*. Inner Mongolia Agricultural University.
- Zhao, S.X., Li, C.Y., Li, C., et al., 2016. Analysis of characteristics of river channel evolution in Inner Mongolia reach of Yellow River based on 3S technology. *Adv. Sci. Technol. Water Resour.* 36 (4), 70–74.
- Zhao, S.X., Li, C.Y., Li, C., et al., 2017. Processes of river ice and ice-jam formation in Shensifenzi Bend of the Yellow River. *J. Hydraul. Eng.* 48 (03), 351–358.
- Zhao, S.X., Shen, H.T., 2021. A laboratory study on seepage flow resistance of ice jams. *J. Hydraul. Eng.* 52 (08), 959–968.
- Zhao, S.-X., Wang, W.-J., Shi, X.-H., Zhao, S.-N., Wu, Y.-J., Quan, Q., Li, C., Szydłowski, M., Li, W., Kolerski, T., 2021. Freeze-up ice jam formation in the river bend, a case study on the Inner Mongolia Reach of Yellow River. *Crystals* 11 (6), 631.